Journal of Polymer Research (2019) 26: 43
https://doi.org/10.1007/s10965-019-1703-y

ORIGINAL PAPER

Effects of β-cyclodextrin complexation of curcumin and quaternization of chitosan on the properties of the blend films for use as wound dressings

Atchara Kaolaor[1] · Sarunya Phunpee[2] · Uracha Rungsardthong Ruktanonchai[2] · Orawan Suwantong[1,3]

Received: 19 August 2018 / Accepted: 8 January 2019 / Published online: 17 January 2019

Abstract

The effects of the β-cyclodextrin (CD) complexation of curcumin (CUR) and the quaternization of chitosan (CS) on the properties of the blend films were studied. The quaternized chitosan containing curcumin (CUR-QCS) and the quaternized β-cyclodextrin grafted with chitosan containing curcumin (CUR-QCD-g-CS) were prepared. The CUR-QCS or CUR-QCD-g-CS was blended with 4% *w/v* of poly(vinyl alcohol) (PVA) and cross-linked with glutaraldehyde to improve the mechanical properties of the blend films. These blend films were characterized for their chemical structure, thermal behaviors, mechanical properties, water swelling, and weight loss. In addition, the release study, antioxidant activity, and indirect cytotoxicity were investigated. From the results, the CUR-QCD-g-CS/PVA films showed higher mechanical properties but lower water swelling and weight loss behaviors than the CUR-QCS/PVA films. In addition, the released amount of CUR from the CUR-QCD-g-CS/PVA films and their antioxidant activity were higher than those from the CUR-QCS/PVA films due to the accommodation of CUR inside CD cavity. Thus, the CD complexation of CUR and the quaternization of CS had an effect on the properties of the blend films.

Keywords Chitosan · β-cyclodextrin · Quaternization · Poly(vinyl alcohol) · Curcumin

Introduction

The current number of people with a chronic wound has steadily increased for each year. Normally, the normal wound healing process occurs through 4 steps: hemostasis, inflammation, proliferation, and remodeling [1]. The chronic wound healing process is more complex than the normal wound healing and needs more time for repairing the damaged tissue. In addition, the key to successful healing the chronic wound is achieving a therapeutic agent concentration at the site of infection. Therefore, the wound dressing is selected for chronic wound healing [2, 3]. The functions of wound dressing are to absorb extracellular fluid with maintaining the moisture of wound, promote tissue regeneration, provide gas exchange, maintain the appropriated temperature for the healing process, and be easily removed [4]. Nowadays, many materials are developed to make the wound dressing materials such as polymers. The polymers are mainly divided into 2 types, natural and synthetic polymers. Natural polymers have a better in biocompatibility, low toxicity, and biodegradability than the synthetic polymers. However, the synthetic polymers show good mechanical properties. Because of the unique properties of the natural and synthetic polymers, various wound dressings are thus made from both types of polymer. Chitosan (CS) is a biomaterial derived from deacetylation of chitin consisting of β-(1,4)-2-amino-2-deoxy-D-glucopyranose unit and β-(1,4)-2-amino-D-glucopyranose units [5, 6]. It is widely studied for various applications due to its non-toxicity, biocompatibility, mucoadhesiveness, and inexpensive biomass [7]. CS also shows the wound healing, antimicrobial, antioxidant, and hemostatic activities which make CS is suitably used in the biomedical fields [7, 8]. Moreover, CS can be fabricated into gels, beads, scaffolds, membranes, films, sponges, nanoparticles, and nanofibers [9].

✉ Orawan Suwantong
o.suwantong@gmail.com

[1] School of Science, Mae Fah Luang University, Chiang Rai 57100, Thailand

[2] National Nanotechnology Center, Thailand Science Park, Pathum Thani 12120, Thailand

[3] Center of Chemical Innovation for Sustainability, Mae Fah Luang University, Chiang Rai 57100, Thailand

β-Cyclodextrin (CD), a group of natural product, consists of seven glucopyranose units linked together by a glycosidic bond. The outer surface of CD shows a hydrophilic property, whereas the central cavity shows a hydrophobic property. Due to the lipophilic central cavities, CD can entrap a variety of hydrophobic guest molecules as a controlled release [10]. Thus, CD can be applied in many fields such as pharmaceuticals [11], cosmetics [12], biotechnology [13], textiles [14], food industry [15], and other industries [16]. Because of the advantages of both CD and CS, thus CS grafted with CD (CD-g-CS) was generated and was used as a carrier material for drug delivery system (Fig. 1a). The combination of CD and CS presents the mucoadhesive property with controlled release property [10]. However, a low water solubility is a limited property of CS. Therefore, the researchers try to modify CS in order to improve the water solubility of CS. Due to the existence of the hydroxyl and amino groups on the molecules, thus CS can be easily modified [17]. Recently, there are many methods to prepare water-soluble CS, such as hydroxyethylacryl chitosan, ethylamine-hydroxyethyl chitosan, carboxymethyl chitosan, and hydroxypropyl chitosan [18–22]. Usually, the water solubility and antibacterial activity of CS can be improved by using quaternary moiety or quaternary agent [17]. Thus, the quaternized chitosan (QCS) with glycidyl trimethylammonium chloride was synthesized. It was found that the QCS derivatives had good water solubility and also had antimicrobial activity [23].

However, the CS films alone have low mechanical properties due to their sensitivity to the environmental condition which limited their applications. Thus, poly(vinyl alcohol) (PVA), which has biocompatibility and biodegradability, was blended with CS films to increase the intermolecular interaction of polymer chains resulting in enhancing the mechanical properties [24–26]. In addition, due to the biocompatibility of CS and PVA, thus their blend films were used in biomedical applications especially in wound dressing and drug delivery system [27]. Curcumin (CUR), a natural polyphenolic compound, is extracted from the rhizomes of *Curcuma longa* L. CUR has many biological activities such as non-toxicity, antioxidant, and anti-inflammatory activities [28]. However, the low water solubility is a major disadvantage of the CUR. As this limited property, several studies have been investigated, such as complexation with CD to enhance the water solubility of CUR. In addition, the complexation of CUR and CD also showed a controlled drug release property due to the interaction between CD cavity and CUR [29].

In this work, the effects of the CD complexation of CUR and the quaternization of CS on the properties of the films were studied. The CUR-QCS/PVA and CUR-QCD-g-CS/PVA films were prepared by a solvent casting method and crosslinked by glutaraldehyde. These blend films were fabricated to use as carriers of CUR and wound dressing materials. These blend films were characterized for their chemical structure, thermal behaviors, mechanical properties, water swelling, weight loss, release characteristics, antioxidant activity, and indirect cytotoxicity.

Experimental

Materials

CS with an average molecular weight of 22 kDa was obtained from Bio 21 Co., Ltd. (Thailand). Acetic acid was purchased from EMSURE (Germany). CD was received from Wacker Chemical AG (Germany). *N,N*-dimethylformamide (DMF)

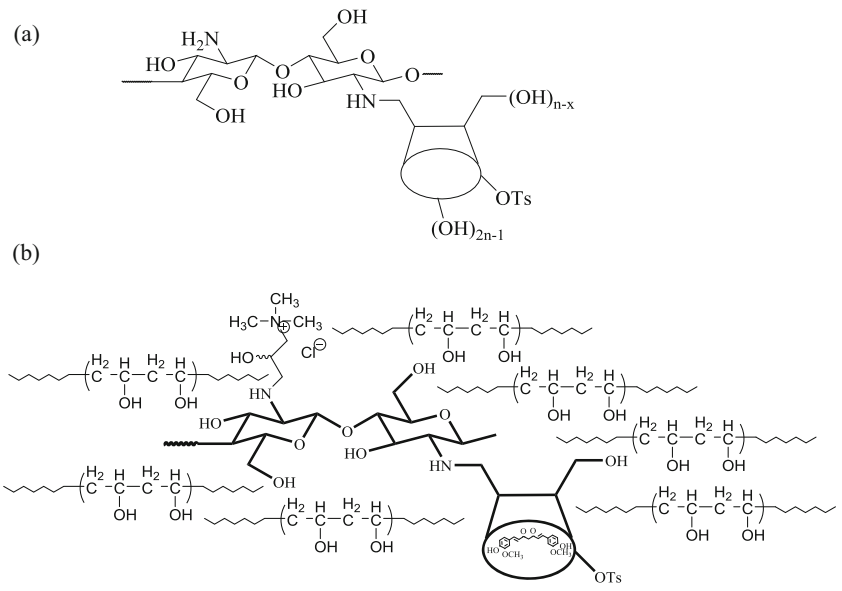

Fig. 1 Chemical structure of CD-g-CS (**a**) and CUR-QCD-g-CS/PVA (**b**)

was purchased from RCI Labscan Co., Ltd. (Thailand). Glycidyl-trimethylammonium chloride (GTMAC) was purchased from Fluka (Switzerland). CUR was purchased from Sigma-Aldrich (Switzerland). Cellulose membrane was purchased from Membrane Filtration Products, Inc. (USA). Dulbecco's Modified Eagle's Medium (DMEM), Fetal Bovine Serum (FBS), and Antibiotic and Antimycotic formulation containing Penicillin G Sodium, Streptomycin Sulfate, and Amphopericin B were purchased from GIBCO, USA. 3-(4,5-dimethylthiazol-2-yl)-2,5-diphenyltetrazolium bromide (MTT) was purchased from AMRESCO (USA).

Preparation of β-cyclodextrin grafted with chitosan (CD-g-CS)

The synthesis of QCD-g-CS was prepared according to the procedure described previously by Gonil et al. [30]. Briefly, O-p-toluenesulfonyl-β-CD (Ts-CD) was synthesized by tosylation of either the primary or secondary sugar hydroxyl groups of CD with p-toluenesulfonyl chloride under basic condition at 0–5 °C. After that, CS solution was prepared by dissolving 1 g of CS in 1% *v*/v acetic acid (80 mL). Then, 3 g of Ts-CD was dissolved in 4 mL of DMF. After that, Ts-CD solution was refluxed with CS solution at 100 °C for 24 h and dialyzed with deionized water using a cellulose membrane (molecular weight cut off 3500 kDa) for 3 days. Finally, the solution was freeze-dried to yield a CD-g-CS cotton.

Preparation of quaternized chitosan (QCS) and quaternized β-cyclodextrin grafted with chitosan (QCD-g-CS)

1 g of CS or CD-g-CS solution was dissolved in 80 mL of 1% *v*/v acetic acid for 24 h and then 6 mL of GTMAC solution was added to the solution. The mixture solution was refluxed at 60 °C for 6 h and then dialyzed with deionized water using a cellulose membrane (molecular weight cut off 3500 kDa) for 3 days. Finally, the solution was freeze-dried to yield a QCS or QCD-g-CS cotton.

Preparation of CUR-QCS/PVA and CUR-QCD-g-CS/PVA films

The CUR-QCS/PVA and CUR-QCD-g-CS/PVA films were prepared by a solvent casting method. The QCS or QCD-g-CS solution was prepared by dissolving QCS or QCD-g-CS in a distilled water at room temperature. While PVA solution was prepared by dissolving PVA powders in a hot distilled water (65 °C) with stirring for 30 min. The blend solution of QCS or QCD-g-CS and PVA solutions (8% *w*/*v*) were mixed together with the weight ratio of 1:1. After that, 2% *w*/w of CUR solution (based on the weight of QCS or QCD-g-CS) was added to the blend solution. The mole ratio of complex inclusion between CUR and CD was 0.2/1. The blend solution was continuously stirred at ambient temperature for 1 h and crosslinked with 0.025% *v*/v of glutaraldehyde solution. Finally, the blend solution was poured into the mold and then dried in an oven at 30 °C for 12 h to obtain the CUR-QCS/PVA or CUR-QCD-g-CS/PVA films.

Characterization

The FTIR spectra of samples were obtained by Perkin Elmer model Spectrum GX. The samples were ground into a powder and mixed with KBr powder. The powder mixture was compressed into a transparent disk and scanned in the range of 4000 to 500 cm^{-1} using the average of 32 scans.

The ^1H NMR spectra of QCS and QCD-g-CS were measured on Nuclear Magnetic Resonance (NMR) Spectrometer 400 MHz (Bruker, Switzerland). All measurements were determined at 673 K with LB parameter of 0.30 Hz using D_2O as the solvent.

X-ray diffraction (XRD) was performed by a PANalytical/X'Pert Pro MPD with CUKα lamp at $\lambda = 1.5406$ A. Diffraction intensity was measured in reflection mode at 5 s scan speed and incensement at 0.01 for $2\theta = 3–40°$.

For the morphological characterization, the surface of each sample was examined coated with a thin layer of gold under vacuum and observed the morphology using a LEO 1450 VP Scanning Electron Microscope (SEM).

Thermal behaviors of samples were investigated using Differential Scanning Calorimetry (DSC, 822e, Mettler Toledo). The samples were heated up at the rate of 5 °C/min from 25 to 600 °C. During the heating, the nitrogen gas was flowed into the furnace at the rate of 60 mL/min.

Mechanical test

The mechanical properties in terms of tensile strength and %elongation at break were investigated by Instron Machine Model 5566 Universal Testing Machine using 1 kN load cell (gauge length = 50 mm and crosshead speed = 10 mm/min). The samples were cut into a 10 cm × 1 cm of rectangular shape and measured at the room temperature. The tensile strength and %elongation at break were calculated from the stress-strain curve using the following equations. The mechanical properties were reported as an average value from three measurements.

$$\text{Tensile strength} = \frac{\text{Maximum Force (N)}}{\text{Area}(\text{mm}^2)} \quad (1)$$

and

$$\%\text{Elongation at break} = \frac{\text{Extension}(\Delta L)}{\text{Original Length}(L)} \times 100 \quad (2)$$

Water swelling and weight loss

The water swelling and weight loss of the CUR-QCS/PVA and CUR-QCD-g-CS/PVA films were examined in phosphate buffer solution (PBS) at 37 °C, for 30 s to 30 min. The measurement of water swelling and weight loss of each sample was calculated by the following equations:

$$\text{Water swelling}(\%) = \frac{M - M_d}{(M_d)} \times 100 \quad (3)$$

and

$$\text{Weight loss}(\%) = \frac{M_i - M_d}{M_i} \times 100 \quad (4)$$

Where M is the weight of each sample after submersion in PBS for specified submersion time. M_d is the weight of each sample after submersion in PBS for specified submersion time in its dry state. M_i is the initial weight of each sample before submersion.

In vitro drug release

Actual curcumin content

The actual amount of CUR in the CUR-QCS/PVA and CUR-QCD-g-CS/PVA films was determined by dissolving the samples in 10 mL of PBS at 37 °C. The sample solution was measured by UV-vis spectrophotometer at the wavelength of 426 nm. The actual amount of CUR in the CUR-QCS/PVA and CUR-QCD-g-CS/PVA films was back-calculated from the calibration curve.

Curcumin release assay

The release characteristics of CUR from the CUR-QCS/PVA and CUR-QCD-g-CS/PVA films were investigated by the total immersion method. Each sample was soaked in 10 mL of PBS at 37 °C for 5 days. After the specified time, the sample solution was withdrawn and replaced with the fresh PBS to maintain the volume. The released amount of CUR from each sample in PBS was investigated by UV-vis spectrophotometer at the wavelength of 426 nm. The amount of released curcumin from the samples at each submersion time points was determined by calculating the received data. The experimental was studied for three times and reported as an average value.

Antioxidant activity

The antioxidant activity of as-released CUR from the CUR-QCS/PVA and CUR-QCD-g-CS/PVA films was investigated with 2,2′-diphenyl-2-picrylhydrazyl (DPPH) radicals, followed to the Blois's method [31]. First, each sample was immersed in PBS at 37 °C for different time points (i.e., 0.5, 1, 5, 15, 60, 300, 600, and 1440 min). The sample solution was withdrawn and then treated with methanolic solution of DPPH (100 μM) for 30 min at room temperature in the dark place. The sample solution was then determined by UV-vis spectrophotometer at the wavelength of 517 nm and the antioxidant activity (%AA) of the as-released CUR was calculated by the following equation:

$$\text{Antioxidant activity}(\%) = \frac{A_{control} - A_{sample}}{A_{sample}} \times 100 \quad (5)$$

Where $A_{control}$ is an observed value of the testing solution without CUR, whereas A_{sample} is an observed value of the testing solution.

Indirect cytotoxicity

The indirect cytotoxicity evaluation of the CUR-QCS/PVA and CUR-QCD-g-CS/PVA films was investigated using Normal Human Dermal Fibroblasts cell line (NHDF; 11th passage) and NCTC clone 929 cells, ATCC® CCL-1™ (3rd passage). The cells were cultured in DMEM, supplemented by 10% FBS and 1% Antibiotic and Antimycotic formulation (containing Penicillin G Sodium, Streptomycin Sulfate, and Amphopericin B) at 37 °C in a humidified atmosphere containing 5% CO_2 for 24 h. The samples were first immersed in serum-free medium (SFM; containing DMEM and 1% Antibiotic and Antimycotic formulation) for 24 h to produce various concentrations of extraction media (i.e., 0.5, 5, and 10 mg/mL) and then sterilized using 0.22 μm Minisart syringe filters (Sartorius, Germany). The NHDF or NCTC clone 929 cells were plated in wells of tissue culture polystyrene (TCPS) at 8,000 cells/well for 24 h to allow cell attachment. The cells were then starved with SFM for 24 h. After that, the medium was replaced with an extraction medium and cells were re-incubated for 24 h. Then, the culture medium in each plate was first removed and washed with 100 μL of phosphate buffered saline. After that, 100 μL of MTT solution (0.5 mg/mL) was added to wells of 96-well TCPS. The plates were then incubated for 2.5 h at 37 °C. After incubation, the solution was removed. 100 μL of DMSO was added to dissolve the formazan crystals. After 10 min of agitation, the absorbance of the solution was measured at the wavelength of 570 nm using an Epoch Microplate Spectrophotometer (BioTek Instruments, USA). The viability of the cells cultured by each of the extraction medium was determined and the viability of the cells cultured by fresh SFM was used as a control.

Statistical analysis

Data were presented as means ± standard errors of means. Statistical analysis was carried out by the one-way analysis of variance (one-way ANOVA) and Tukey's post hoc test in SPSS (IBM SPSS, USA). The statistical significance was accepted at $p < 0.05$.

Results and discussion

Synthesis and characterization of CUR-QCS/PVA and CUR-QCD-g-CS/PVA films

The chemical structures of CD-g-CS and CUR-QCD-g-CS/PVA are shown in Fig. 1. CS showed the characteristic FTIR pattern at the wavenumber of 3441 cm^{-1} due to OH and NH_2 groups. The absorption peaks at the wavenumber of 1657 and 1151 cm^{-1} were attributed to C=O and C-O stretching of the amide group, whereas the absorption peak at the wavenumber of 1595 cm^{-1} was due to the vibration of the amine group. Moreover, CS showed the absorption band in the range of 1082-1032 cm^{-1} corresponding to the symmetric stretching of C-O-C (Fig. 2). The FTIR spectra of Ts-CD exhibited the additional absorption peaks at the wavenumber of 1644 and 1157 cm^{-1} corresponding to the C=C stretching of the aromatic group and S=O stretching of the sulfonyl group, respectively, while the CD-g-CS exhibited the absorption peak of the CD and CS at the wavenumber of 1599 cm^{-1} corresponding to the vibration of the amine group while the absorption peak at the wavenumber of 1154 cm^{-1} corresponding to the S=O

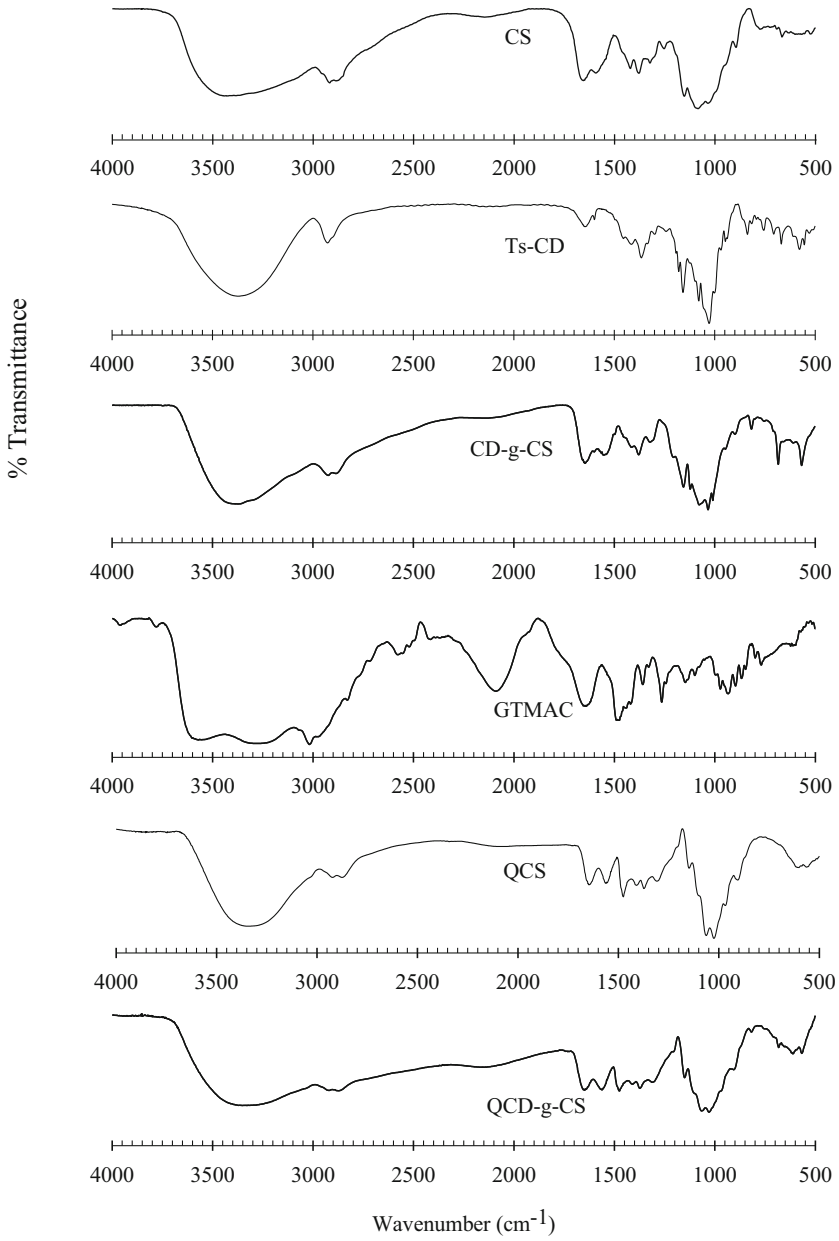

Fig. 2 FTIR spectra of CS, Ts-CD, CD-g-CS, GTMAC, QCS and QCD-g-CS

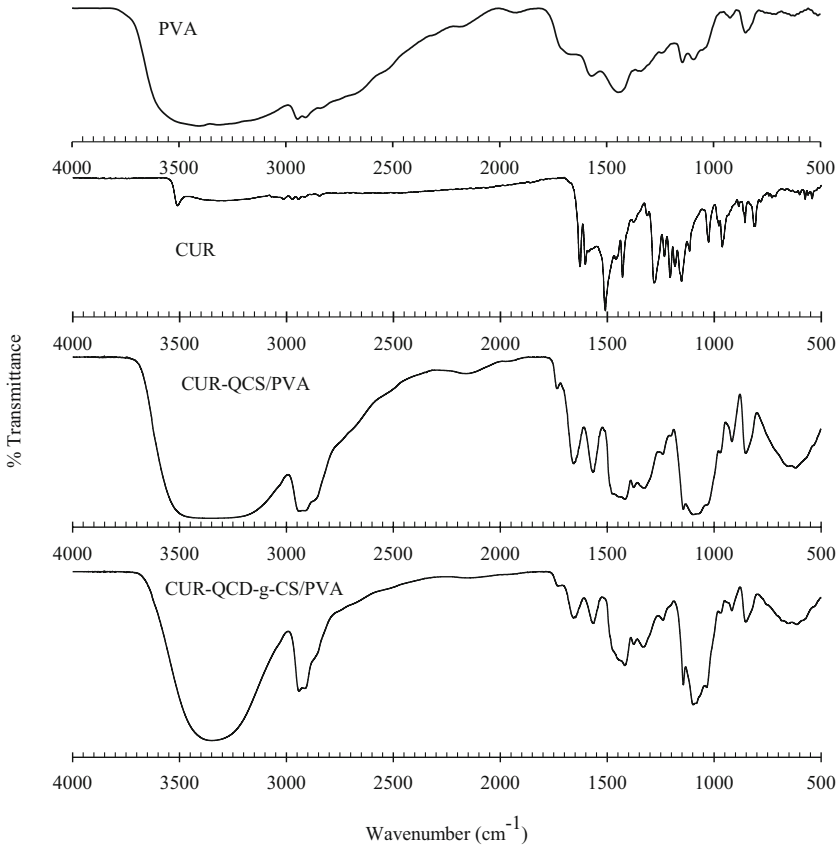

Fig. 3 FTIR spectra of PVA, CUR, CUR-QCS/PVA, and CUR-QCD-g-CS/PVA

stretching of the sulfonyl group. The wavenumber in the range of 1119–1010 cm^{-1} corresponded to the symmetric stretching of the C-O-C and skeleton vibration of the C-O stretching. The QCS and QCD-g-CS exhibited the characteristic FTIR spectra at the wavenumber of 1473 cm^{-1} due to the C-H stretching of the methyl substituent of the quaternary ammonium groups [30].

Figure 3 shows the FTIR spectra of PVA, CUR, CUR-QCS/PVA and CUR-QCD-g-CS/PVA. The FTIR pattern of PVA appeared at 3400 and 2947 cm^{-1} corresponding to -OH stretching vibration [32]. For CUR, the characteristic FTIR pattern showed at the wavenumber of 1280 cm^{-1} due to the C-O stretching vibration of the benzene ring. The characteristic FTIR patterns of the CUR-QCS/PVA and CUR-QCD-g-CS/PVA films showed a board peak at 3352 cm^{-1} which attributing to the overlapped O-H and N-H stretching. Moreover, the CUR-QCS/PVA and CUR-QCD-g-CS/PVA films showed the absorption peak at 1280 cm^{-1} corresponding to the C-O stretching from CUR. In summary, various typical peaks of the samples were shifted indicating that each component was blended together excellently.

Figure 4 shows the ^{1}H NMR spectra of QCS and QCD-g-CS. The ^{1}H NMR spectrum of QCS showed the proton signal at δ 3.1 and 2.6 ppm corresponding to the quaternary

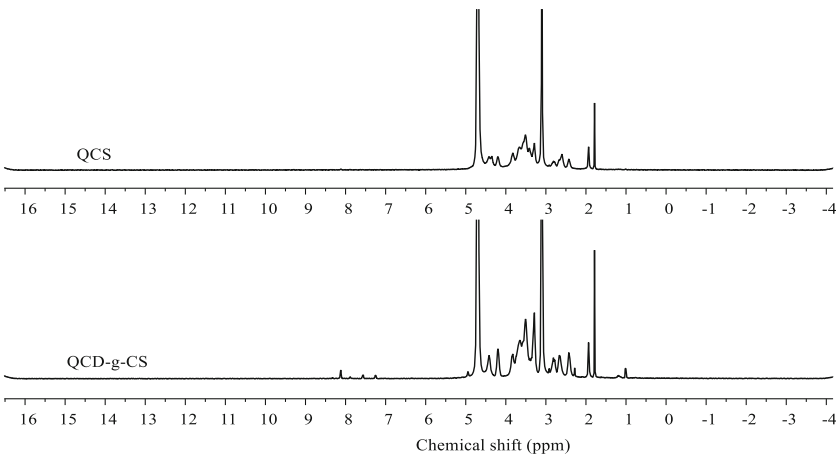

Fig. 4 ^{1}H NMR spectra of QCS and QCD-g-CS

ammonium proton and methylene proton. Moreover, the proton signal at 2.9 was corresponded to the proton of CS. Similarly, the QCD-g-CS spectrum showed the doublet protons at δ 7.6–7.2 ppm corresponding to aromatic protons of Ts group on CD. The proton signal at δ 4.9 ppm was assigned to the proton of CD. Moreover, the proton signal at δ 3.1 was corresponded to quaternary ammonium proton and the protons signal at 2.6 was corresponded to methylene proton.

Figure 5 shows the XRD patterns of CS, QCS, QCD-g-CS, PVA, CUR-QCS/PVA, and CUR-QCD-g-CS/PVA. The XRD pattern of CS showed 3 characteristic peaks around 2θ = 10.4°, 20°, and 22.4°. The reflection appeared at 2θ = 10.4° corresponding to crystal form I, while the reflection appeared at 2θ = 20° corresponding to crystal form II. Compared with CS, the broad single XRD patterns of QCS and QCD-g-CS were observed indicating that the crystallinity of samples was decreased. The decrease in crystallinity could be the presence of quaternary ammonium group might obstruct the formation of inter- and extra-molecular hydrogen bonding of CS backbone [31]. For PVA, the XRD pattern exhibited sharp crystalline reflection at 2θ = 19.89° corresponding to crystalline atactic PVA and a shoulder at 2θ = 22.9° [33]. CUR showed the characteristic peaks at 2θ = 8.03°, 9.11°, 12.37°, 14.76°, 17.55°, 2147°, 25.65°, and 19.11°, etc. corresponding to CUR crystalline nature. While the CUR-QCD-g-CS/PVA film exhibited the characteristic peak of CUR at 2θ = 14.01° and 17.31°. These results suggested that the CUR might form an inclusion complex with CD. Moreover, the decreasing in the number of peaks indicated that the crystallinity might change into amorphous form [34].

SEM images of the surface of QCS/PVA, QCD-g-CS/PVA, CUR-QCS/PVA, and CUR-QCD-g-CS/PVA films are shown in Fig. 6. From the results, the blending of QCS and QCD-g-CS with PVA with and without CUR showed the uniform and smooth surface without aggregates and pores. Thus these results indicated that there was no phase separation meaning that the quaternized CS derivatives and CUR molecules had the uniform distribution into the PVA matrix.

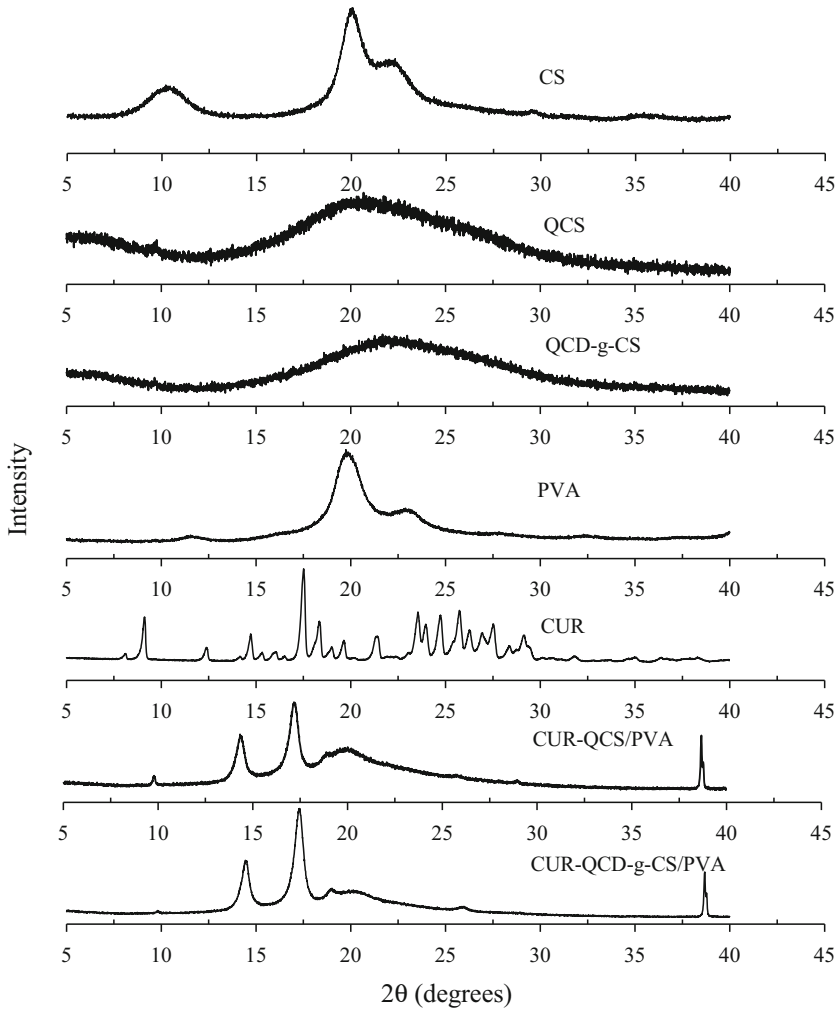

Fig. 5 XRD patterns of CS, QCS, QCD-g-CS, PVA, CUR, CUR-QCS/PVA, and CUR-QCD-g-CS/PVA

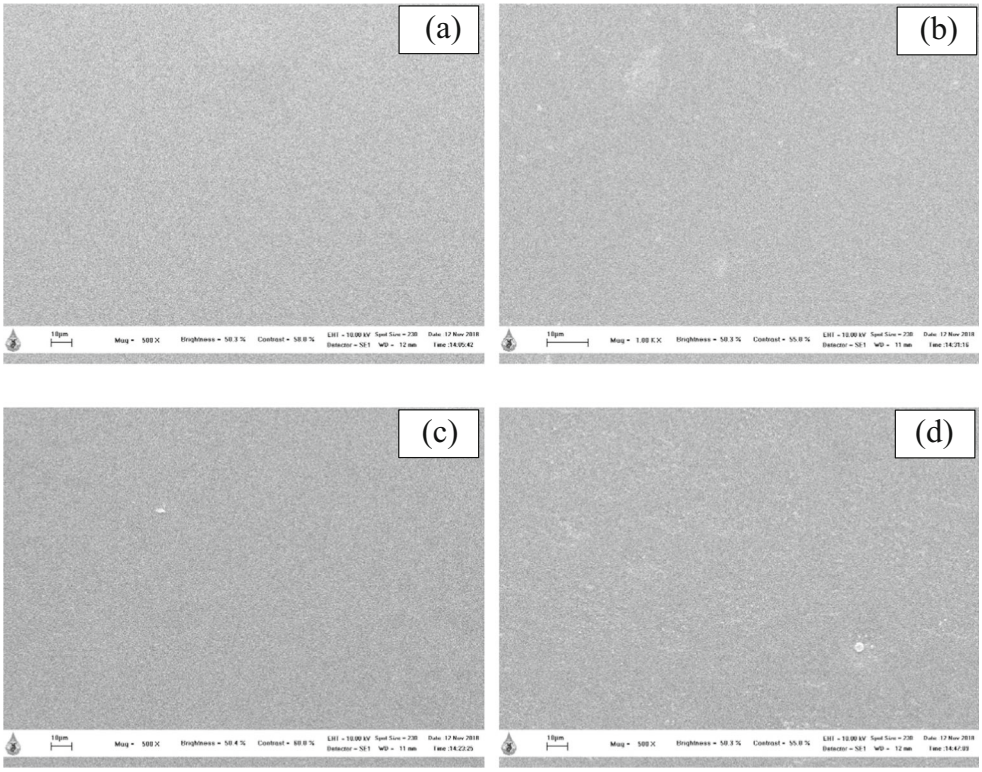

Fig. 6 SEM images of QCS/PVA (**a**), QCD-g-CS/PVA (**b**), CUR-QCS/PVA (**c**), and CUR-QCD-g-CS/PVA films

Figure 7 shows thermal behaviors of CUR, CUR-QCS-PVA, and CUR-QCD-g-CS/PVA. The DSC thermogram of CUR showed endothermic peak at 321 °C due to its melting point. While the endothermic peak of CUR-QCS/PVA and CUR-QCD-g-CS/PVA films at 321 °C was completely disappeared. These results can be concluded that the CUR molecules were included in the CD cavity on CS backbone.

Mechanical properties of CUR-QCS/PVA and CUR-QCD-g-CS/PVA films

The mechanical properties including tensile strength and elongation at break of the CUR-QCS/PVA and CUR-QCD-g-CS/PVA films were investigated and the results are shown in Table 1. The tensile strength and elongation at break of the CUR-QCS/PVA films were ~19 MPa and

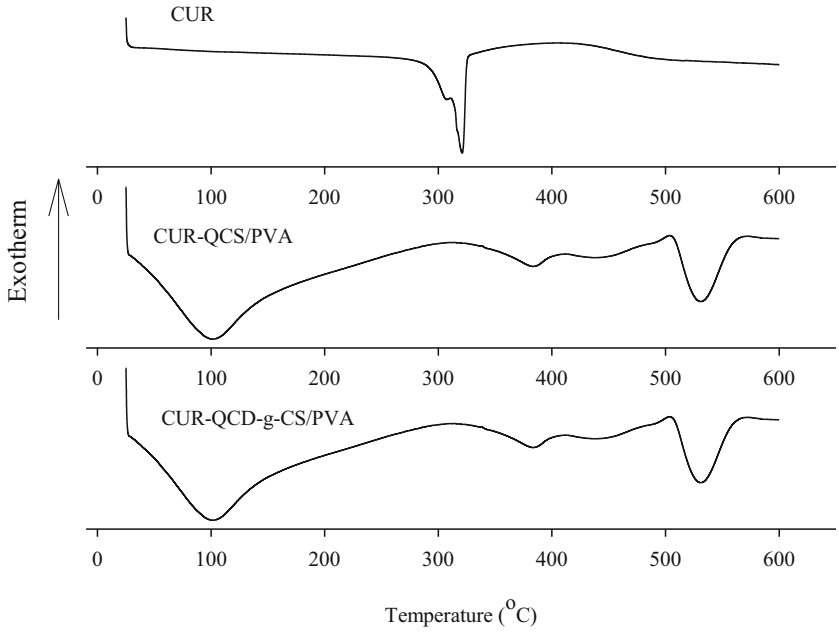

Fig. 7 DSC thermograms of CUR, CUR-QCS/PVA, and CUR-QCD-g-CS/PVA

Table 1 Mechanical properties of the CUR-QCS/PVA and CUR-QCD-g-CS/PVA films

Type of quaternized chitosan films	Tensile strength (MPa)	Elongation at break (%)
CUR-QCS/PVA	18.75 ± 3.78	75.67 ± 12.39
CUR-QCD-g-CS/PVA	22.62 ± 3.49	234.89 ± 35.34*

*$p < 0.05$ compared with the CUR-QCS/PVA film

~757%, respectively, while the tensile strength and elongation at break of the CUR-QCD-g-CS/PVA films were ~23 MPa and ~235%, respectively. These results were reported as the effect of the hydrogen bonding between glutaraldehyde crosslinking and the bulky group of the quaternized salt. The interaction of glutaraldehyde with both hydroxyl groups of PVA and the residual of amino groups from CS produced a true hydrogen bonding. However, the quaternized salt, the bulky group that grafted on CS chains, decreased the hydrogen bonding by increasing the space between the polymer chains resulting in low tensile strength of CUR-QCS/PVA films. Moreover, the bulky group of the quaternary ammonium salt reduced the movement of the polymer chains resulting in lower elongation at break of the CUR-QCS/PVA films [35].

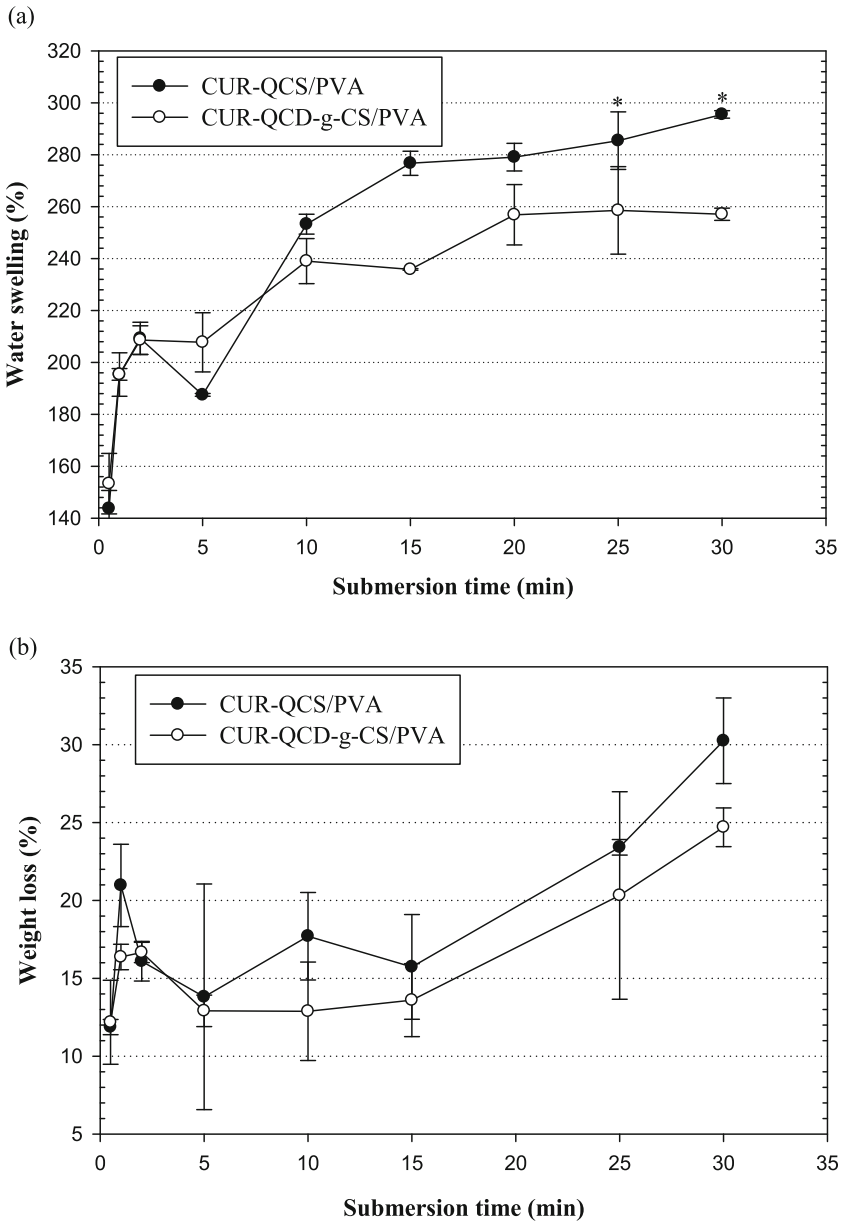

Fig. 8 **a** Water swelling and **b** weight loss of the CUR-QCS/PVA and CUR-QCD-g-CS/PVA films. $p < 0.05$ compared with the CUR-QCS/PVA films

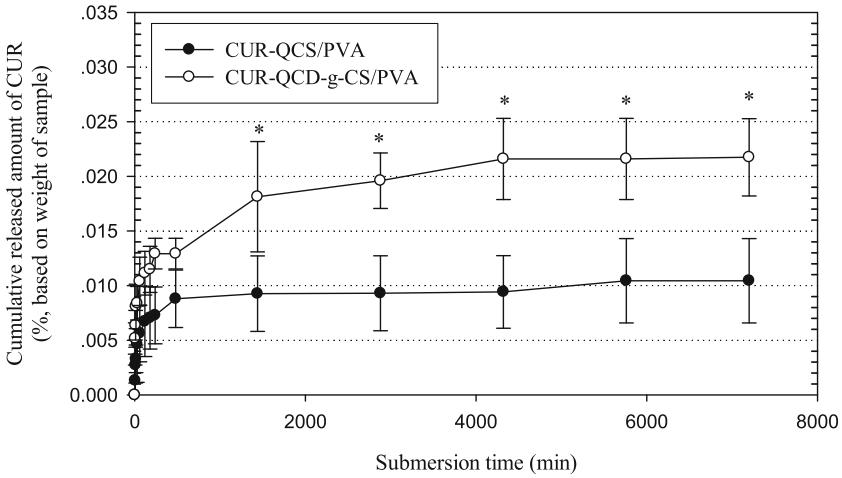

Fig. 9 Cumulative release profiles of CUR from the CUR-QCS/PVA and CUR-QCD-g-CS/PVA films. $p < 0.05$ compared with the CUR-QCS/PVA films

Water swelling and weight loss behaviors of CUR-QCS/PVA and CUR-QCD-g-CS/PVA films

The CUR-QCS/PVA and CUR-QCD-g-CS/PVA films were further characterized to determine their swelling capability and weight loss behaviors after submersion in PBS (pH 7.4) at 37 °C. From Fig. 8a, the water swelling of both the CUR-QCS/PVA and CUR-QCD-g-CS/PVA films increased with increasing submersion time. Comparing between the CUR-QCS/PVA and CUR-QCD-g-CS/PVA films, the water swelling of the CUR-QCD-g-CS/PVA films was lower than that of the CUR-QCS/PVA films after submersion for 10–25 min. This result might be due to the presence of higher water soluble group or quaternary ammonium group at the primary amino groups on CS chains of QCS. The loss in the weight of the CUR-QCS/PVA and CUR-QCD-g-CS/PVA films was also investigated and the results are shown in Fig. 8b. The weight loss of both the CUR-QCS/PVA and CUR-QCD-g-CS/PVA films increased with increasing submersion time. The CUR-QCS/PVA films exhibited the greater water swelling and weight loss behaviors than the CUR-QCD-g-CS/PVA films. These results might be the substitution of CD on CS backbone resulted in the reduction of the primary amino group of CS where the quaternary ammonium can be grafted [30].

Release study of CUR from CUR-QCS/PVA and CUR-QCD-g-CS/PVA films

The actual amount of CUR in the CUR-QCS/PVA and CUR-QCD-g-CS/PVA films was investigated before investigating the release characteristic of CUR from the blend films. The actual amount of CUR contained in both the CUR-QCS/PVA and CUR-QCD-g-CS/PVA films was 0.00021 and 0.00011 mg/mg (based on the weight of samples), respectively. These values were further used to investigate the release characteristics of CUR from the blend films.

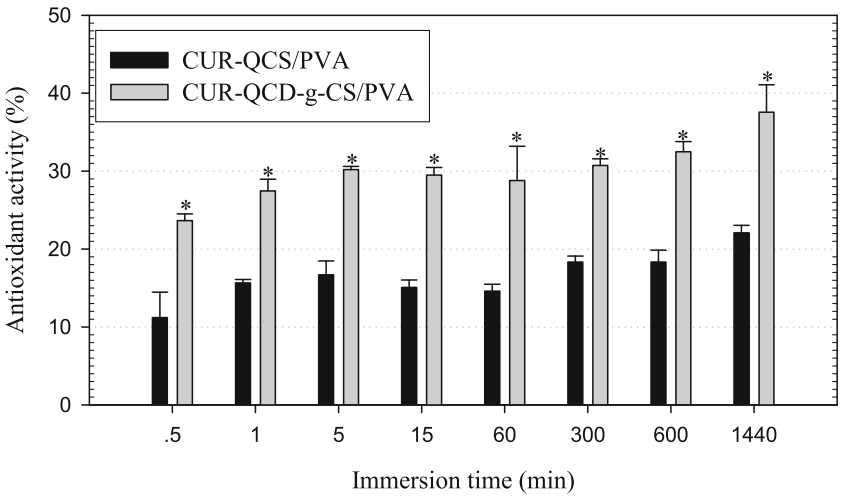

Fig. 10 Antioxidant activity of the released CUR from the CUR-QCS/PVA and CUR-QCD-g-CS/PVA films. $p < 0.05$ compared with the CUR-QCS/PVA films

The release characteristics of CUR from both the CUR-QCS/PVA and CUR-QCD-g-CS/PVA films were studied in PBS (pH 7.4) at 37 °C. From Fig. 9, both the CUR-QCS/PVA and CUR-QCD-g-CS/PVA films showed an initial burst release which can be attributed to CUR attach on the outer surface of the films and followed by a sustained release up to the 7200 min. The released amount of CUR from the CUR-QCD-g-CS/PVA films was higher than that from the CUR-QCS/PVA films because of the higher water solubility of CD accommodating CUR inside.

Antioxidant activity

The antioxidant activity of the as-released CUR from both the CUR-QCS/PVA and CUR-QCD-g-CS/PVA films was investigated by DPPH assay. These results were represented by the ability of CUR to deactivating the DPPH radicals. As expected, the antioxidant activity of the as-released CUR from the CUR-QCD-g-CS/PVA films after submersion from 0.5 to 1440 min was higher than the CUR-QCS/PVA films with significant results (Fig. 10). This might be due to the complexation of CUR in the CD cavity resulting in the higher release amount of CUR. These results were supported by Kono et al. They reported that the prepared CD grafted with CS hydrogels exhibited the absorption properties toward acetylsalicylic acid (ASA) due to the presence of CD in the structure. In addition, the amount of ASA absorbed into the hydrogels was enhanced with an increase in the amount of CD incorporated within the hydrogels [36].

Indirect cytotoxicity

The indirect cytotoxicity evaluation of the CUR-QCS/PVA and CUR-QCD-g-CS/PVA films was investigated to evaluate the potential use of these films as wound dressing materials. From Fig. 11, the viability of NHDF cells cultured with the extraction media from these films compared with the cells cultured with the fresh culture medium ranged between 11 and 114%. While the viability of NCTC clone 929 cells cultured with the extraction media with different extraction ratios ranged between 13 and 105%. According to ISO 10993-5 in vitro cytotoxicity standard states that "reduction of cell viability by more than 30% is considered a cytotoxic effect". From these results, the viability of both NHDF and NCTC clone 929 cells cultured with the extraction media at only concentration of 0.5 mg/mL was higher than 70%. Thus, these blend films might not be toxic to both NHDF and NCTC clone 929 cells. However, these films should be treated with 0.1 M glycine solution before further testing in cell culture.

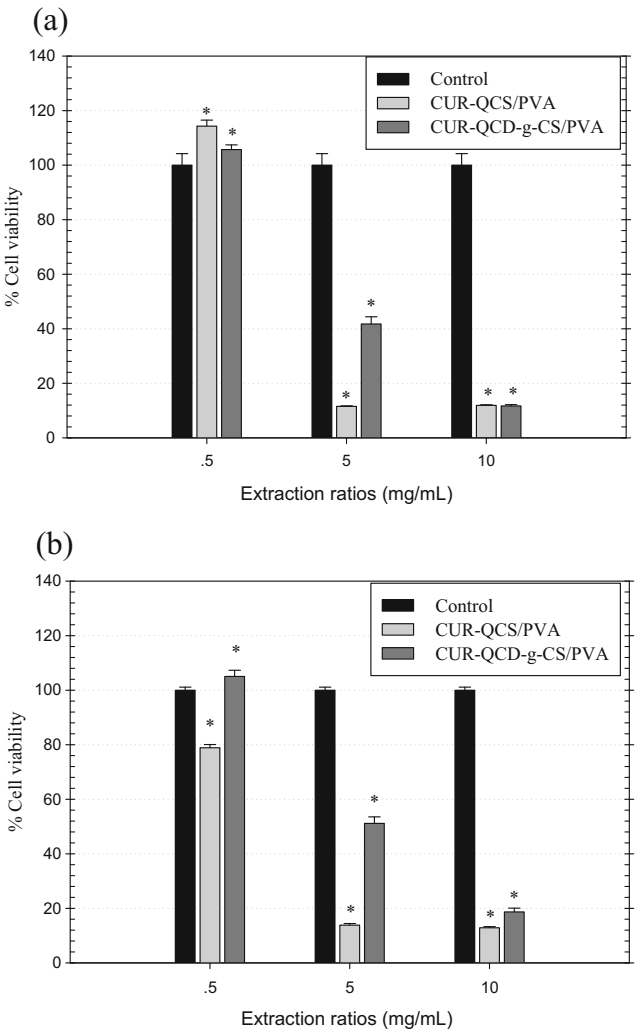

Fig. 11 Indirect cytotoxicity of the CUR-QCS/PVA and CUR-QCD-g-CS/PVA films cultured with **a** NHDF cells and **b** NCTC clone 929 cells. $p < 0.05$ compared with fresh culture medium

Conclusion

In summary, the grafting of CS with CD (CD-g-CS) was successfully synthesized. The substitution of CD to the CS backbone resulted in the reduction of the primary amino group of CS. Thus, the quaternary ammonium salt was grafted on the free primary amino group. The quaternization of CS and CD-g-CS with GTMAC increased the water solubility of the films. The CUR-QCD-g-CS/PVA films showed higher mechanical properties but lower water swelling and weight loss behaviors. In addition, the released amount of CUR from the CUR-QCD-g-CS/PVA films and their antioxidant activity were higher than those from the CUR-QCS/PVA films due to the accommodation of CUR inside the CD cavity. For indirect cytotoxicity, the viability of both NHDF and NCTC clone 929 cells cultured with the extraction media

at only concentration of 0.5 mg/mL was higher than 70% indicating these films might be non-toxic to the cells.

Acknowledgments The authors would like to acknowledge the Research and Researchers for Industries-RRI M.Sc. scholarship (MSD60I0010) and Jinnaluck Co., Ltd., the National Science and Technology Development Agency (NSTDA) and Mae Fah Luang University.

References

1. Morton LM, Phillips TJ (2016) Wound healing and treating wounds: differential diagnosis and evaluation of chronic wounds. J Am Acad Dermatol 74:589–605
2. Erfurt-Berge C, Renner R (2015) Chronic wounds–recommendations for diagnostics and therapy. Rev Vasc Med 3: 5–9
3. Frieri M, Kumar K, Boutin A (2016) Wounds, burns, trauma, and injury. Wound Med 13:12–17
4. Dhivya S, Padma VV, Santhini E (2015) Wound dressings-a review. Biomedicine 5:22
5. Tsigos I, Martinou A, Kafetzopoulos D, Bouriotis V (2000) Chitin deacetylases: new, versatile tools in biotechnology. Trends Biotechnol 18:305–312
6. Yen MT, Yang JH, Mau JL (2009) Physicochemical characterization of chitin and chitosan from crab shells. Carbohydr Polym 75: 15–21
7. Pandey AR, Singh US, Momin M, Bhavsar C (2017) Chitosan: application in tissue engineering and skin grafting. J Polym Res 24:215
8. Yen MT, Yang JH, Mau JL (2008) Antioxidant properties of chitosan from crab shells. Carbohydr Polym 74:840–844
9. Anitha A, Sowmya S, Sudheesh Kumar PS, Deepthi S, Chennazhi KP, Ehrlich H, Tsurkan M, Jayakumar R (2014) Chitin and chitosan in selected biomedical applications. Prog Polym Sci 39:1644–1667
10. Venter JP, Kotzé AF, Auzély-Velty R, Rinaudo M (2006) Synthesis and evaluation of the mucoadhesivity of a CD-chitosan derivative. Int J Pharm 313:36–42
11. Ijaz M, Matuszczak B, Rahmat D, Mahmood A, Bonengel S, Hussain S, Huck CW, Bernkop-Schnürch A (2015) Synthesis and characterization of thiolated β-cyclodextrin as a novel mucoadhesive excipient for intra-oraldrug delivery. Carbohydr Polym 132:187–195
12. Centini M, Maggiore M, Casolaro M, Andreassi M, Facino RM, Anselmi C (2007) Cyclodextrins as cosmetic delivery systems. J Incl Phenom Macrocycl Chem 57:109–112
13. Singh M, Sharma R, Banerjee UC (2002) Biotechnological applications of cyclodextrins. Biotechnol Adv 20:341–359
14. Cireli A, Yurdakul B (2006) Application of cyclodextrin to the textile dyeing and washing processes. J Appl Polym Sci 100:208–218
15. Astray G, Gonzalez-Barreiro C, Mejuto JC, Rial-Otero R, Simal-Gándara J (2009) A review on the use of cyclodextrins in foods. Food Hydrocoll 23:1631–1640
16. Del Valle EMM (2004) Cyclodextrins and their uses: a review. Process Biochem 39:1033–1046
17. Zhu D, Chen H, Li J, Zhang W, Shen Y, Chen S, Ge Z, Chen S (2016) Enhanced water-solubility and antibacterial activity of novel chitosan derivatives modified with quaternary phosphonium salt. Mat Sci Eng C 61:79–84
18. Ma G, Yang D, Zhou Y, Xiao M, Kennedy JF, Nie J (2008) Preparation and characterization of water-soluble *N*-alkylated chitosan. Carbohydr Polym 74:121–126
19. Xie Y, Liu X, Chen Q (2007) Synthesis and characterization of water-soluble chitosan derivate and its antibacterial activity. Carbohydr Polym 69:142–147
20. Hu Y, Peng J, Ke L, Zhao D, Zhao H, Xiao X (2016) Alginate/carboxymethyl chitosan composite gel beads for oral drug delivery. J Polym Res 23:129
21. Anitha A, Divya Rani VV, Krishna R, Sreeja V, Selvamurugan N, Nair SV, Tamura H, Jayakumar R (2009) Synthesis, characterization, cytotoxicity and antibacterial studies of chitosan, *O*-carboxymethyl and *N,O*-carboxymethyl chitosan nanoparticles. Carbohydr Polym 78:672–677
22. Peng Y, Han B, Liu W, Xu X (2005) Preparation and antimicrobial activity of hydroxypropyl chitosan. Carbohydr Res 340:1846–1851
23. Jia Z, Shen D, Xu W (2011) Synthesis and antibacterial activities of quaternary ammonium salt of chitosan. Carbohydr Res 333:1–6
24. Koyano T, Koshizaki N, Umehara H, Nagura M, Minoura N (2000) Surface states of PVA/chitosan blended hydrogels. Polymer 41: 4461–4465
25. Chuang WY, Young TH, Yao CH, Chiu WY (1999) Properties of the poly (vinyl alcohol)/chitosan blend and its effect on the culture of fibroblast in vitro. Biomaterials 20:1479–1487
26. Chandy T, Sharma CP (1992) Prostaglandin E_1-immobilized poly (vinyl alcohol)-blended chitosan membranes: blood compatibility and permeability properties. J Appl Polym Sci 44:2145–2156
27. Rafique A, Zia KM, Zuber M, Tabasum S, Rehman S (2016) Chitosan functionalized poly (vinyl alcohol) for prospects biomedical and industrial applications: a review. Int J Biol Macromol 87: 141–154
28. Ghosh S, Banerjee S, Sil PC (2015) The beneficial role of curcumin on inflammation, diabetes and neurodegenerative disease: a recent update. Food Chem Toxicol 83:111–124
29. Popat A, Karmakar S, Jambhrunkar S, Xu C, Yu C (2014) Curcumin-cyclodextrin encapsulated chitosan nanoconjugates with enhanced solubility and cell cytotoxicity. Colloids Surf B Biointerfaces 117:520–527
30. Gonil P, Sajomsang W, Ruktanonchai UR, Pimpha N, Sramala I, Nuchuchua O, Saesoo S, Chaleawleart-umpon S, Puttipipatkhachorn S (2011) Novel quaternized chitosan containing β-cyclodextrin moiety: synthesis, characterization and antimicrobial activity. Carbohydr Polym 83:905–913
31. Blois MS (1958) Antioxidant determinations by the use of a stable free radical. Nature 181:1199–1200
32. Madera-Santana TJ, Freile-Pelegrín Y, Azamar-Barrios JA (2014) Physicochemical and morphological properties of plasticized poly (vinyl alcohol)–agar biodegradable films. Int J Biol Macromol 69: 176–184
33. Ricciardi R, Auriemma F, De Rosa C, Lauprêtre F (2004) X-ray diffraction analysis of poly (vinyl alcohol) hydrogels, obtained by freezing and thawing techniques. Macromolecules 37:1921–1927
34. Yadav VR, Suresh S, Devi K, Yadav S (2009) Effect of cyclodextrin complexation of curcumin on its solubility and antiangiogenic and anti-inflammatory activity in rat colitis model. AAPS PharmSciTech 10:752–762
35. Mohamed RR, Elella MHA, Sabaa MW (2015) Synthesis, characterization and applications of N-quaternized chitosan/poly (vinyl alcohol) hydrogels. Int J Biol Macromol 80:149–161
36. Kono H, Teshirogi T (2015) Cyclodextrin-grafted chitosan hydrogels for controlled drug delivery. Int J Biol Macromol 72: 299–308